Structural Engineering and Mechanics, Vol. 10, No. 2 (2000) 139-156
DOI: http://dx.doi.org/10.12989/sem.2000.10.2.139

A study of dynamic responses of incorporating damaged materials and structures

Wohua Zhang†, Yunmin Chen† and Yi Jin‡

Institute of Geotechnical Engineering, Zhejiang University, Hangzhou, 310027, China

Abstract. This paper concerns the development of a computational model for the damage evolution of engineering materials under dynamic loading. Two models describing the anisotropic damage evolution of a material are presented; the first is based on a power function of the effective equivalent stress and the second on the damage strain energy release rate. The methods for computing the damage accumulated in structural components and their implementation in a finite element programme are presented together with some numerical results. The dynamic response of a damaged structural component and the dynamic behaviour of a damaged material have been studied numerically. This study shows that the frequency spectrum of a damaged structure is down-shifted, while the damping ratio of damaged materials becomes higher, the amplitude of the response significantly increases and the resonance ensuing from the damage growth still occurs in a damaged structure.

Key words: dynamic response; damage evolution law; damage-based FEM analysis.

1. Introduction

When a structural component is subjected to impact or dynamic loading, its response can cause an elevation of the stress level especially in a damaged zone or in the region surrounding a crack or a defect. In particular, the micro structure of the material within the damaged zone is significantly changed compared to its undamaged state, due to the activation and growth of the damage. As a result, for example, the frequency decreases and both the damping ratio and the amplitude increase.

During damage evolution, the macroscopic properties of the material change too (Cordebois and Sidoroff 1982, Marigo 1985). In most cases, the deviation from the elastic response derives from the nucleation of new micro-cracks and the growth of existing micro-cracks. So it can be said that the non-linear behaviour of such materials arises as a consequence of the irreversible changes of the microstructure, which is what happens in a damage process (Fahrenthold 1991, Kachanov 1986).

Hence when analysing damage-mechanics problems, not only the damage initiation, growth and failure of a structure need to be taken into consideration, but a number of other mechanical properties of the material also need to be looked at (Zhang 1993, Zhang and Valliappan 1998). These properties may include elastic modulus, ultimate strength, yield stress, fatigue limit, creep rate, damping ratio and heat conductivity. The effects on these properties may be even more significant in cases of anisotropic damage (Cordebois 1982, Zhang and Valliappan 1990).

† Professor
‡ Senior Engineer

In the present study, Audoin and Baste developed a specific ultrasonic device by evaluation of stiffness tensor changes due to anisotropic damage in a ceramic matrix composite in order to identify damage in a material (Audoin and Baste 1994). Pandey and Biswas developed an analytical model for detecting and locating damages in structures using changes in flexibility matrix (Pandey and Biswas 1994). Gamby *et al*. (Gamby 1997) presented a model to predict non-uniform development of damage induced by kinematic wave in composite laminates.

It is of paramount importance in Civil Engineering to be able to predict the effects of damage on the frequency and dynamic characteristics of a structure, especially under dynamic loading. To this end, the dynamic response of a damaged structural component and the dynamic behavior of a damaged material are dealt with this paper within a continuum damage-mechanics approach.

From the numerical examples presented here, it was found that the dynamic loading applied to a damaged structure, leads to a significant growth and propagation of the damage, to a reduction of the natural frequencies of the system and to a state of resonance. In studying the properties of the damaged materials, it was found that the damping ratio increased significantly, whereas the equivalent viscous damping and critical damping decreased, owing to damage growth.

2. Finite element equations of a damaged body

The concept of anisotropic damage can be considered in two cases, the first is in an isotropic material, the second is in an anisotropic material. Thus, the anisotropy in damaged materials may be resulted only from the anisotropic damage in the first case or both by the anisotropic damage and the anisotropy of material in the second case. The term of anisotropy in this study is considered in the second case if without special indication.

The finite element equation representing an anisotropcally damaged body can be presented as

$$[M]\{\ddot{U}\}+[C^*(\Omega(t))]\{\dot{U}\}+[K^*(\Omega(t))]\{U\}=\{P(t)\} \tag{1}$$

where $[M]=\int_{V_e}\rho[N]^T[N]dv$ is the mass matrix for a damaged element, $[K^*(\Omega(t))]=\int_{V_e}[B]^T[T_\sigma]^T[\hat{D}^*][T_\sigma][B]dv$ is the time dependent stiffness matrix for an anisotropically damaged element, $\{P(t)\}=\int_{S_2}[N]^T\{Q(t)\}ds+\int_{V_e}[N]^T\{F(t)\}dv$ is known as the general nodal force vector, $[C^*(\Omega(t))]$ is the time-dependent damping matrix.

In the elastic case, the constitutive matrix of an anisotropically damaged material at a given point and time in a general coordinate system ($\boldsymbol{xyz}$) can be presented as:

$$[D^*]=[T_\sigma]^T[\hat{D}^*][T_\sigma] \tag{2}$$

Where $[\hat{\boldsymbol{D}}^*]$ is the elastic matrix of anisotropically damaged material in the principal coordinates of the anisotropy ($\boldsymbol{x}_1$, $\boldsymbol{x}_2$, $\boldsymbol{x}_3$) (Valliappan, Zhang and Murti 1990). In 2-D, the elastic anisotropically damaged material can be expressed as

$$[\hat{D}^*]=\begin{bmatrix} \frac{E_1(1-\Omega_1)^2}{1-\nu_{12}\nu_{21}} & \frac{E_2(1-\Omega_1)(1-\Omega_2)\nu_{12}}{1-\nu_{12}\nu_{21}} & 0 \\ \frac{E_2(1-\Omega_2)(1-\Omega_1)\nu_{21}}{1-\nu_{12}\nu_{21}} & \frac{E_2(1-\Omega_2)^2}{1-\nu_{12}\nu_{21}} & 0 \\ 0 & 0 & \frac{2G_{12}(1-\Omega_1)^2(1-\Omega_2)^2}{(1-\Omega_1)^2+(1-\Omega_2)^2} \end{bmatrix} \tag{3}$$

The anisotropically-damaged state of a material in 3-D can be expressed by the anisotropic damage vector $\{\Omega\}=\{\Omega_1, \Omega_2, \Omega_3\}^T$, where the principal anisotropic damage variables, $\Omega_1, \Omega_2, \Omega_3$, are the principal values of a second order tensor of damage. The matrix $[T_\sigma]$ in Eq. (2) is the coordinate stress vector transformation matrix defined in 2-D as

$$[T_\sigma]=\begin{bmatrix} \cos^2\theta & \sin^2\theta & -\sin2\theta \\ \sin^2\theta & \cos^2\theta & \sin2\theta \\ 0.5\sin2\theta & -0.5\sin2\theta & \cos2\theta \end{bmatrix} \tag{4}$$

in which θ is the two dimensional anisotropic orientation angle.

The relationship between the net (effective) stress vector $\{\boldsymbol{\sigma}^*\}$ and the Cauchy stress vector $\{\boldsymbol{\sigma}\}$ for anisotropically damaged materials in the global coordinate system (***xyz***) can be presented as

$$\{\sigma^*\}=[\Phi^*]\{\sigma\} \tag{5}$$

where $[\Phi^*]$ is the damage transfer matrix (Zhang and Valliappan 1998), which has the following formulation in 2-D (plane stress):

$$[\Phi^*]=\begin{bmatrix} \frac{\cos^2\theta}{1-\Omega_1}+\frac{\sin^2\theta}{1-\Omega_2} & 0 & \left(\frac{1}{1-\Omega_1}-\frac{1}{1-\Omega_2}\right)\frac{\sin2\theta}{2} \\ 0 & \frac{\sin^2\theta}{1-\Omega_1}+\frac{\cos^2\theta}{1-\Omega_2} & \left(\frac{1}{1-\Omega_1}-\frac{1}{1-\Omega_2}\right)\frac{\sin2\theta}{2} \\ \left(\frac{1}{1-\Omega_1}-\frac{1}{1-\Omega_2}\right)\frac{\sin2\theta}{2} & 0 & \frac{\sin^2\theta}{1-\Omega_1}+\frac{\cos^2\theta}{1-\Omega_2} \\ 0 & \left(\frac{1}{1-\Omega_1}-\frac{1}{1-\Omega_2}\right)\frac{\sin2\theta}{2} & \frac{\cos^2\theta}{1-\Omega_1}+\frac{\sin^2\theta}{1-\Omega_2} \end{bmatrix} \tag{6}$$

Since the micro-structure within a material has changed due to damage, the material constants and the internal energy dissipation (internal damping) also change (Zhang 1993). Therefore, the stiffness matrix and the damping matrix of a damaged element must be considered as a function of the damage variable $\{\boldsymbol{\Omega}\}$ which varies with time. Strictly speaking, the mass density will also change due to the damage. However, from the point of view of mass conservation, the global mass is unchanged, and a mass matrix independent of the damage has to be assumed. On the other hand, damage causes a stiffness degradation, and the frequency spectrum of the structure is down-shifted significantly. Hence, the damage has inevitable influences on the internal damping.

So far, the influence of damage on material damping has not been the subject of any major experimental or analytical investigation. In order to discuss this problem from the point of view of numerical analysis, it is convenient to assume a Rayleigh-type damping and the equivalent viscous damping.

For the Rayleigh damping matrix, one can adopt the usual formulation:

$$[C^*(\Omega(t))]=\alpha^*[M]+\beta^*[K^*(\Omega(t))] \tag{7}$$

For the equivalent viscous damping matrix, we have

$$[C^*(\Omega(t))]=\int_{V_e} r^*(t)[N]^T[N]dv \tag{8}$$

where α^*, β^* are the Rayleigh damping parameters of the damaged material, and $\boldsymbol{r}^*(t)$ is the time-dependent equivalent viscous damping coefficient.

3. Damage evolution equation

For the complete analysis of dynamic damage, it is necessary to introduce the damage kinetic equation (Kachanov 1986) of the form

$$\dot{\Omega}=\dot{\Omega}(\sigma_{ij}, \Omega, ...) \tag{9}$$

It means that the damage growth rate is related to the state of stress and damage, which means - in other words- that the damage and the stresses distributed in an element are a function of time and position (for example in 2-D, $\boldsymbol{\sigma_{ij}(x, y, t)}$, $\boldsymbol{\Omega(x, y, t)}$). The time and space integration of the damage kinetic equations in a F. E. analysis is hence difficult (Kachanov 1986, and Zhang 1992).

Most previous investigations considered the damage kinetic equation to be in the form of a power law (Kachanov 1986, Marigo 1985). So far, two major damage evolution criteria have been proposed for different kinds of materials. The first is a power function of an equivalent stress and the other is based on the damage strain-energy release rate (Valliappan and Zhang 1996, Zhang and Valliappan 1998). Both criteria have been applied in this study. In the case of anisotropy, the kinetic equation can be represented as

$$\frac{d\Omega_i}{dt}=\begin{cases} A\left(\dfrac{\sigma_{eq}}{1-\Omega_i}\right)^n & \sigma_{eq}\geq\sigma_{di} \\ 0 & \sigma_{eq}<\sigma_{di} \end{cases} \tag{10}$$

and

$$\frac{d\Omega_i}{dt}=\begin{cases} B\bar{Y}^k & Y_i>Y_{di} \\ 0 & Y_i\leq Y_{di} \end{cases} \tag{11}$$

where $\boldsymbol{A} > \mathbf{0}$, $\boldsymbol{n} > \mathbf{0}$ in Eq. (10) are material constants whose values depend on the rate of loading. $\boldsymbol{A}$ and $\boldsymbol{n}$ can be evaluated by experiments, based on the three point test (Fahrenthold 1991, Gamby 1997). The parameters $\boldsymbol{B} > \mathbf{0}$, $\boldsymbol{k} > \mathbf{0}$ in Eq. (11) are material constants, which as well as $\boldsymbol{A}$ and $\boldsymbol{n}$, can be determined by experimental measurements using a procedure similar to that already presented (Fahrenthold 1991). σ_{eq} can be considered as an equivalent stress based on a failure criterion, such as von Mises, Mohr-Coulomb or Drucker-Prager (Zhang 1992, Zhang and Valliappan 1998). $\boldsymbol{\sigma_{di}}$ is the threshold value of the tensile stress at the onset of damage growth in the $\boldsymbol{i}$-th direction. The total damage strain energy release rate $\boldsymbol{Y}$ can be expressed (Zhang 1992, Valliappan and Zhang 1996, Zhang and Valliappan 1998) as

$$\bar{Y} = Y_1 + Y_2 + Y_3 = \frac{1}{2}\{\sigma\}^T [T_\sigma]^T [d^*][T_\sigma]\{\sigma\} \tag{12}$$

where Y_i is the damage strain-energy release rate in the $\boldsymbol{i}$-th anisotropic direction. Y_{di} in Eq. (11) is the threshold value of the damage strain-energy release rate in the $\boldsymbol{i}$-th anisotropic direction at the start of damage growth

$$Y_i = -\frac{1}{2}\{\sigma\}^T [T_\sigma]^T \frac{\partial [D^*]^{-1}}{\partial \Omega_1} [T_\sigma]\{\sigma\} \tag{13}$$

$$[d^*] = \sum_{i=1}^{3} \frac{\partial [D^*]^{-1}}{\partial \Omega_i} = \begin{bmatrix} d_{11}^* & d_{12}^* & d_{13}^* & 0 & 0 & 0 \\ d_{21}^* & d_{22}^* & d_{23}^* & 0 & 0 & 0 \\ d_{31}^* & d_{32}^* & d_{33}^* & 0 & 0 & 0 \\ 0 & 0 & 0 & g_{23}^* & 0 & 0 \\ 0 & 0 & 0 & 0 & g_{31}^* & 0 \\ 0 & 0 & 0 & 0 & 0 & g_{12}^* \end{bmatrix} \tag{14}$$

in which

$$d_{ij}^* = \frac{2}{(1-\Omega_i)^3 E_i} \qquad i \le 3 \tag{15}$$

$$d_{ij}^* = \frac{((1-\Omega_i) + (1-\Omega_j))\nu_{ij}}{(1-\Omega_i)^2 (1-\Omega_j)^2 E_i} \qquad i \ne j,\ i \le 3\ j \le 3 \tag{16}$$

$$g_{ij}^* = \frac{(1-\Omega_i)^3 + (1-\Omega_j)^3}{(1-\Omega_i)^3 (1-\Omega_j)^3 G_{ij}} \qquad i \ne j,\ i \le 3\ j \le 3 \tag{17}$$

The integration of Eqs. (10) and (11) can be carried out using the Newmark scheme for the accumulation of damage increments over Δt intervals at each Gaussian point in an element.

4. Damping for damaged material

For the Rayleigh damping defined in Eq. (7), the damaged damping ratio ζ^* corresponding to the ***i***-th order vibration mode of a damaged structure can be written in similar manner to that for the undamaged case as

$$\zeta_i^* = \frac{1}{2}\left(\frac{\alpha^*}{\omega_i^*} + \beta^* \omega_i^*\right) \tag{18}$$

where ω_i^* is the ***i***-th circular frequency of a damaged structure.

The contribution of higher order modes to the dynamic response of a structure is less significant than the contribution of the first and second modes. Hence, the dynamic response can be approximated using only the first- and second-order damping ratios. In the case of isotropic damage, a simple relationship can be found from Eq. (18) and the relation $\omega_i^* = (1-\Omega)\omega_i$ if the Rayleigh damping parameters α and β are assumed to be constant.

$$\zeta_i^* = \frac{1}{2}\left(\frac{\alpha}{(1-\Omega)\omega_i} + (1-\Omega)\beta\omega_i\right) \tag{19a}$$

$$\zeta_i = \frac{1}{2}\left(\frac{\alpha}{\omega_i} + \beta\omega_i\right) \tag{19b}$$

The Rayleigh damping parameters α and β can be approximately measured by a specified frequency of a mode such as by the first or the second frequency as ($\alpha \approx \zeta_1\omega_1$, $\beta \approx \zeta_1/\omega_1$ or $\alpha \approx \zeta_2\omega_2$, $\beta \approx \zeta_2/\omega_2$) (Wang 1993). The ratio of β/α can be estimated more accurately by the geometry mean from both modes and formulated independently to the damping ratio as $\beta/\alpha \approx 1/(\omega_1\omega_2)$. On the other hand, the parameters α and β can be approximately measured also by two frequencies ω_1, ω_2 and a specified damping ratio ζ as $\alpha \approx 2\omega_1\omega_1\zeta/(\omega_1+\omega_1)$ and $\beta \approx 2\zeta/(\omega_1+\omega_1)$ (Wang 1993), the ratio β/α gives the same results as $\beta/\alpha \approx 1/(\omega_1\omega_2)$. Therefore, a ratio of damaged to undamaged damping ratios $\eta_\zeta = \zeta^*/\zeta$ can be defined as a function of the damage variable Ω and of the ratio between the natural frequencies ω_1/ω_2 of the corresponding undamaged structure;

$$\eta_\zeta = \frac{\zeta^*}{\zeta} = \frac{\dfrac{1}{1-\Omega} + (1-\Omega)\dfrac{\omega_1}{\omega_2}}{1 + \dfrac{\omega_1}{\omega_2}} \tag{20}$$

Since the ratio of the natural frequency ω_1/ω_2 is known when the geometrical and physical parameters of a structure are given, Eq. (20) can describe the influence of damage on the material damping of a damaged structure. Therefore, η_ζ can be defined as "the Damping-Ratio Damage Factor" (Valliappan and Zhang 1993, Zhang and Valliappan 1998). Eq. (20) combined with Eq. (18) can be used to evaluate the damping ratio ζ^* of damaged materials. Thus, the damaged Rayleigh damping parameters α^*, β^* can be approximately determined after obtaining the damaged frequency ω_1^*/ω_2^*

$$\alpha^* = \frac{2\omega_1^*\omega_2^*}{\omega_1^* + \omega_2^*}\zeta^* \tag{21}$$

$$\beta^* = \frac{2}{\omega_1^* + \omega_2^*}\zeta^* \tag{22}$$

Introducing the equivalent viscous damping (Meirovitch 1975) for damaged and undamaged materials by

$$\gamma^* = 2\overline{m}\,\omega^*\zeta^* \tag{23}$$

$$\gamma = 2\overline{m}\,\omega\zeta \tag{24}$$

where $\overline{m}$ is equivalent mass. The ratio of damaged to undamaged equivalent viscous damping can be written as

$$\eta_\gamma = \frac{\gamma^*}{\gamma} = (1-\Omega)\eta_\zeta = \frac{1 + (1-\Omega)^2\dfrac{\omega_1}{\omega_2}}{1 + \dfrac{\omega_1}{\omega_2}} \tag{25}$$

5. Dynamic behaviour of damaged structures

5.1. Response of damaged structure under dynamic loading

The dynamic response of a damaged structure can be obtained by means of numerical solutions and analytical solutions. If the damage state within a damaged material under dynamic loading has unstable characteristics, then the response of the damaged structure should be coupled with the damage growth. For an unstable damage state, the determination of the dynamic response as mentioned above must combine the Eqs. (11) and (12) with the governing Eq. (1).

In order to clearly and directly illustrate the effect of damage on the dynamic behavior of materials and the dynamic response of damaged structures, in the present study, simple cantilever beams, simply-supported deep beams (in the isotropic case) and simply-supported shell plates (in the orthotropic case) have been studied numerically. The purpose of these analyses is to simulate

Table 1 Structural geometry and material properties of analyzed components

Structural geometry			Material properties					
Type	Size	Load	E1~E2 Mpa	ν_{12}	ρ Kg/m^3	ζ	A~B	n~k
Cantilever beam	25 × 1 × 1 (m)	Concentrated at free end	1.0×10^5 1.0×10^5	0.3	1.0	0.01		
Simple supported deep beam	50 × 6 × 2.5 (mm)	Concentrated at center	2.76×10^7 2.76×10^7	0.22	3600	0.02	4.2×10^{-52} 2.49×10^8	22 11
Simple supported squall plate	2 × 2 × 0.2 (m)	Distributed uniform	54.2 13.6	0.26	1.0	0.01		

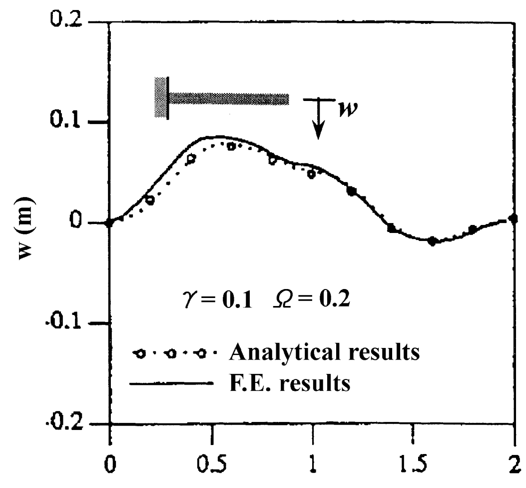

Fig. 1 Response at free end of the damaged cantilever beam

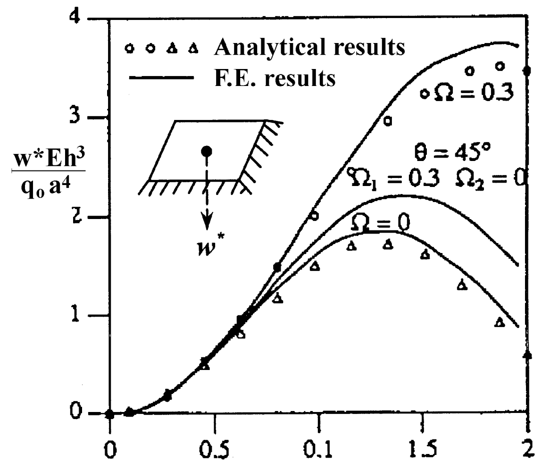

Fig. 2 Dynamic response at the center of the damaged square plate

some experimental tests on damaged structures subject to dynamic loading. The structural geometry and material properties are given in Table 1.

In this study, the analysis of the dynamic response is based on the direct numerical-integration method in the time domain. From the analysis, it should be noted that the results from different integration schemes (for example the Newmark and Wilson θ schemes) do not differ significantly under the corresponding integration stability conditions for various damage states.

Figs. 1 and 2 numerically compare the analytical solutions (Meirovitch 1975, Zhang 1992) for the dynamic responses in cases of isotropic damage (ν=0.3, E_2/E_1=1, Ω=0.3 and γ=1.0) and orthotropic (anisotropic) damage (Ω_1=0.3, Ω_2=0, θ=45°). The dynamic response results plotted in Fig.(1) are for the cantilever beam with damage state Ω=0.2 and viscous damping parameter γ=0.1.

The results presented in Fig. 2 are dimensionless, and results for an undamaged plate are also shown in Fig. 2. The analytical results are obtained only for the isotropic damage case using the Laplace transformation technique and the numerical results are obtained for both isotropic and anisotropic damage cases using the Newmark time integration technique.

The responses presented in Figs. 1 to 5 simulate the deflection at the loading point of the structure under unit rectangular pulse loading over non-dimensional time, where w is the deflection at the loading point of the structure and T is the length of the first period of time when the structure is undamaged.

In order to illustrate the influence of damage evolution on the dynamic response of a damaged structure, a dimensionless plot of the ratio of damaged and undamaged maximum displacements for different representations of damage state is shown in Figs. 3 and 4 for the damaged cantilever beam. Fig. 3 shows the ratio of damaged and undamaged maximum displacement at the free end of the cantilever beam against the degree of damage. Fig. 4 shows the ratio of damaged and undamaged maximum displacement at the free end of the cantilever beam versus the ratio of length of the damaged zone to the whole length of the cantilever beam as the damage zone spreads from the fixed and to the free end.

It is evident that the maximum displacement increases significantly with damage growth and

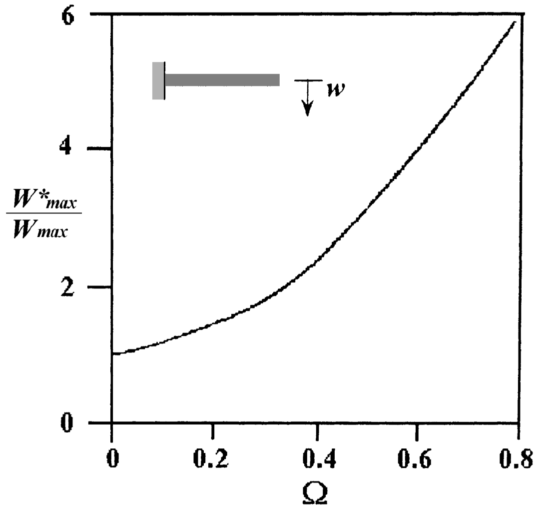

Fig. 3 Ratio of the damaged and undamaged maximum response against the degree of damage

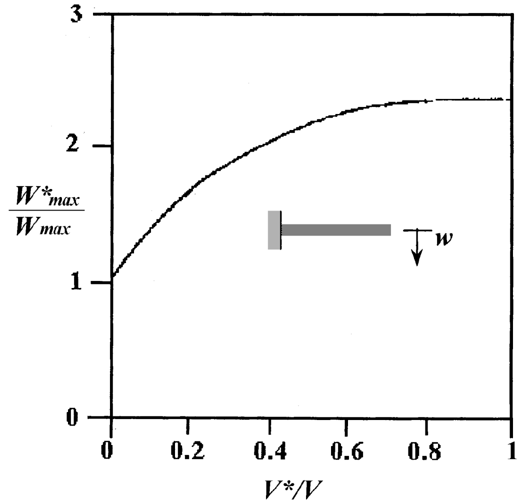

Fig. 4 Ratio of the damaged and undamaged maximum responses against the proportion of the damaged volume in the beam

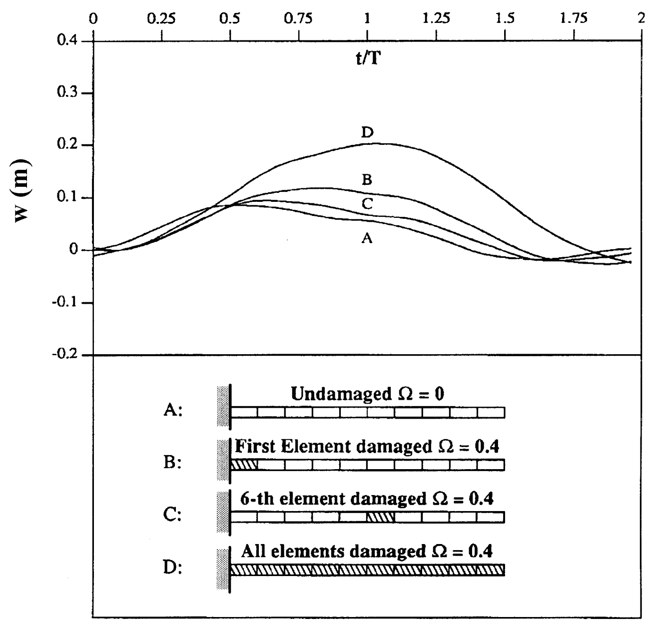

Fig. 5 Effect of location of damaged element in the beam on the dynamic response

propagation. It can be seen that the value of the ratio is as high as 6 when the damage variable is 0.8. Fig. 3 can be used to illustrate the effect of the damage variable on the maximum deflection of the damaged cantilever beam. Fig. 4 can be used to observe the effect of damage propagation on the maximum deflection of the damaged cantilever beam. This phenomenon is defined as the concept of Damage Propagation (i.e., damage zone expansion) in damage mechanics to distinguish it from the concept of Damage Growth (i.e., damage value increases) (Kachanov 1986).

Fig. 5 indicates the effect of the location of the damaged element on the deflection at the free end of the beam as a function of the non-dimensional time. It can be observed from the dynamic response of the structure that the location of the damage is very significant comparing cases B and C for example, it can be seen that the response when the damage is located at the fixed end has more effect than that when located at the middle element.

5.2. Damage evolution during dynamic response

Figs. 6 and 7 are plots of the dynamic response based on two different damage evolution laws, under impact loading. As Figs. 6 and 7 show, the displacements and equivalent stress increase with damage evolution when compared with the case of no damage.

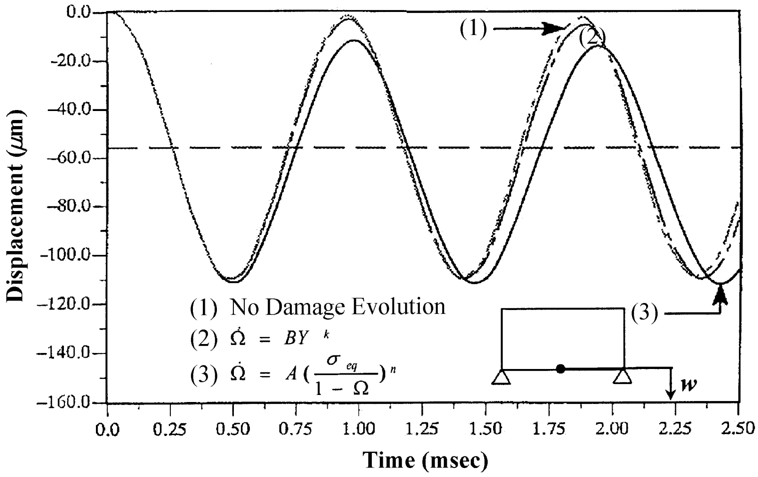

Fig. 6 Vertical displacement of the node at the bottom and middle section during damage evolution

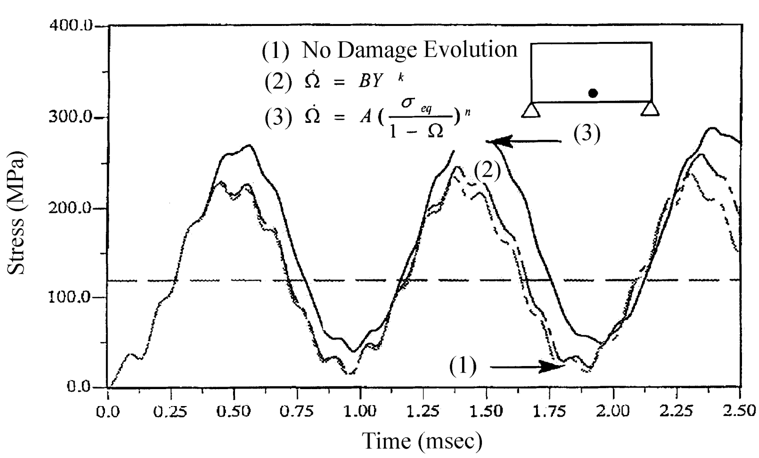

Fig. 7 Average net von-Mises equivalent stress in the element at the bottom and middle beam during damage evolution

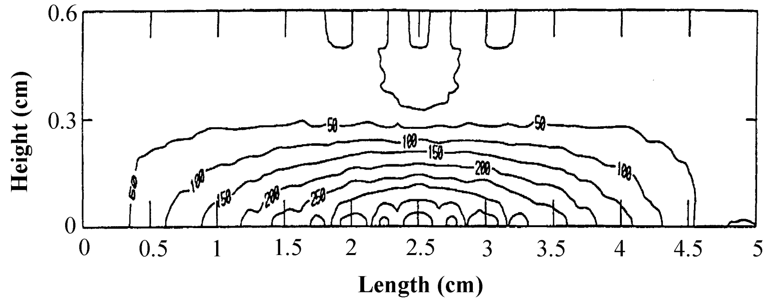

Fig. 8 Major net principal stress contour in MPa at time t=0.445 (msec) during damage evolution

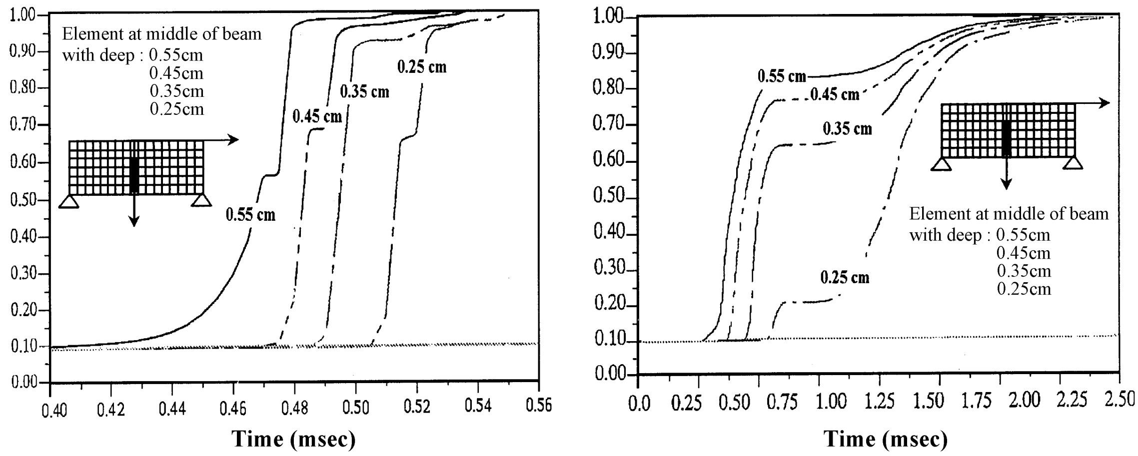

(a) : Model $\dot{\Omega} = BY^k$ (b): Model $\dot{\Omega} = A(\sigma_{eq}/(1-\Omega))^n$

Fig. 9 Averaged damage in an element in the central section and at different depths in the beam during damage evolution with initial damage of 0.09

Numerical comparisons of the different damage evolution models indicate that the power function damage evolution law based on the equivalent stress gives a faster damage growth-rate than damage evolution based on the damage strain-energy release rate. But, when there are pre-existing micro-cracks, the latter damage evolution law gives a much greater damage value during loading due to the factor of $(1-\Omega)^3$ in Eq. (15).

In Fig. 8, the major principal stress contours at time $t = 0.445$ msec (at which the maximum values of stress occur) are shown. It can be observed that the elements close to the middle section of the deep beam are more stressed than the others and hence the damage grows very rapidly at that section.

Figs. 9(a) and (b) show damage evolution in the elements located in the central section and at different depths in the beam, when there is an initial average damage of 0.09 in all elements. The plots in Figs. 9(a) and (b) indicate the duration history of the averaged damage in each element for the two different damage growth models respectively.

It should be pointed out again that in the case of zero initial damage, the damage in each element grows faster when the damage evolution is based on an equivalent stress than in the case of damage strain-energy release rate. The maximum value of the average damage at time $t = 2.5$ (msec) is

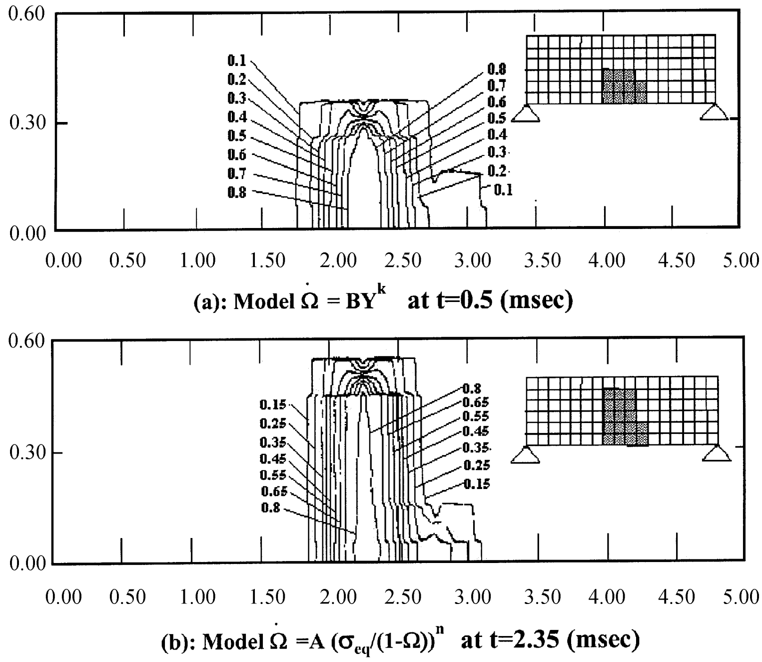

Fig. 10 Average damage contour with initial damage Ω=0.09

0.155 for the damage strain-energy release rate model, and 0.32 for the equivalent stress model.

The damage evolution law of $d\Omega/dt=BY^k$ is very sensitive to an initial damage. That is the specimen fails faster than for the equivalent stress case. This fact has been illustrated in Figs. 9(a) and (b). Although elements fail from time $t=0.44$ to 0.50 (msec) according to $d\Omega/dt=BY^k$, the beam carries the load until t becomes 0.52 to 0.56 (msec). But using $d\Omega/dt=A\ (\sigma_{eq}/(1-\Omega))^n$, the beam carries the load until time t=2.355 (msec).

In Figs. 10(a) and (b), the average damage contours according to the two different damage evolution laws have been plotted. The damage mainly grows in the central zone of the beam because of the greater stress concentration there.

6. Influence of damage on dynamic behavior

6.1. Influence of damage on frequency of damaged structure

The influence of damage on the natural frequencies of a continuum system has been studied using both analytical and numerical analysis. The numerical results were obtained through eigenvalue analysis using the Subspace Recurrence Method.

The analytical and FE solutions are compared in Figs. 11 to 13. Fig. 11 compares numerical FE solution of the period T^* for the degree of damage in the cantilever beam with the solution of eigenvalue analysis for various damage levels Ω=0~0.8. In Figs. 12 and 13, the ratios of frequencies between damaged and undamaged cases are presented for the square plate, both by analytical and finite element solutions.

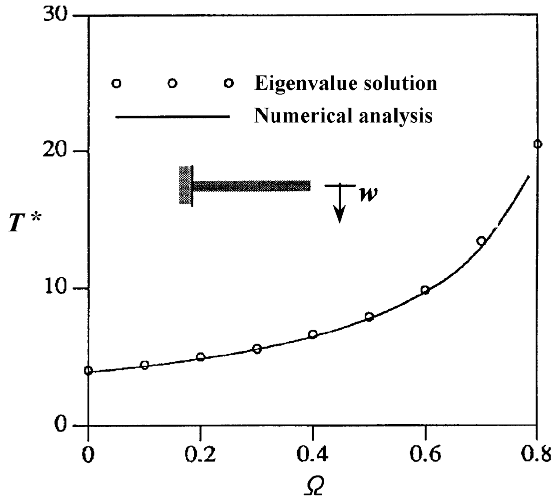

Fig. 11 Period T^* of the damaged cantilever beam versus damage

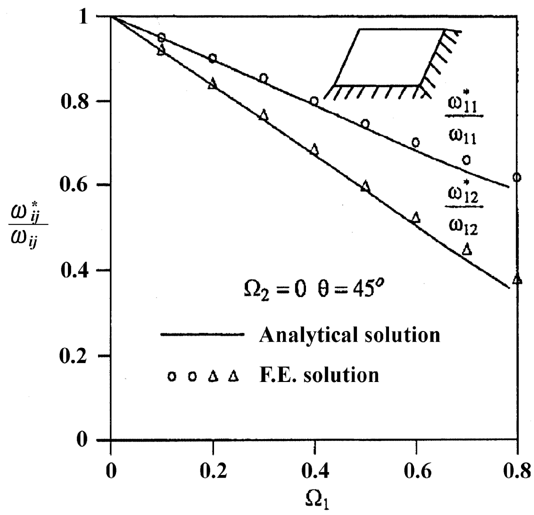

Fig. 12 Frequency ratio of damaged and undamaged plate versus damage Ω_1

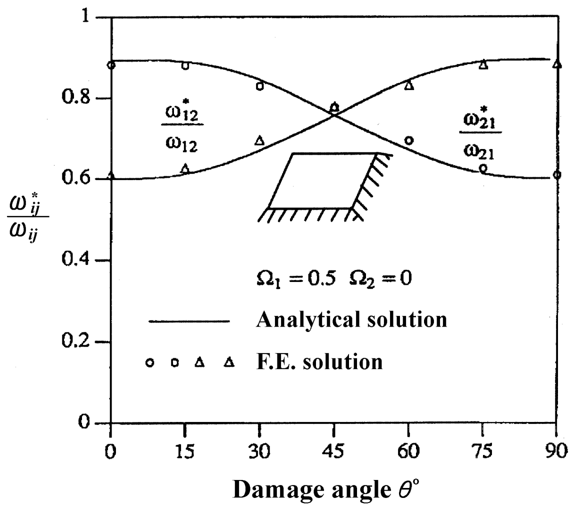

Fig. 13 Frequency ratio of damaged and undamaged plate versus damage angle θ

Fig. 12 shows the frequency ratio $\omega_{ij}^*/\omega_{ij}$ for the damaged and undamaged square plate as the damage variable Ω_1 varies from 0 to 0.8 simulated for the case of $\theta = 45^o$ and Ω_2=0. Fig. 13 shows the cross frequency ratio ($\omega_{ij}^*/\omega_{ij}$ $i \neq j$) for the damaged and undamaged square plate as the damage angle θ varies from 0^o to 90^o simulated for the case of Ω_1=0.5, Ω_2=0. It can be seen from these figures that the results of FE analysis compare well with the analytical results.

The influence of damage on the diagonal frequency ratio ($\omega_{ii}^*/\omega_{ii}$ i=j) and the cross frequency ratio ($\omega_{ij}^*/\omega_{ij}$ $i \neq j$) between damaged and undamaged cases as the damage variable changes is presented for three vibration modes.

It is interesting to note from Figs. 12 and 13 that the frequencies for higher modes are 'down-shifted' by a larger amount than that for the lower modes. This phenomenon conforms to the

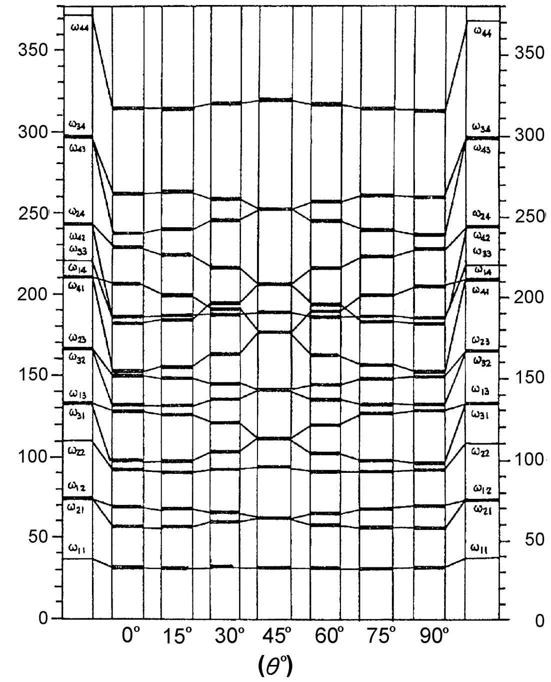

Fig. 14 Influence of anisotropic damage angle θ on frequency spectrum of the damaged square plate

frequency shift trend illustrated also in Fig. 14.

Fig. 14 illustrates the influence of the anisotropic damage angle θ on the frequency spectrum of the square plate. It can be seen that the form of down-shifted frequency for different damage angles θ is quite regular, and the variation of frequency spectrum is symmetric about $\theta = 45^{\circ}$. All frequencies have been down-shifted significantly by anisotropic damage. Whereas, the influence of the damage angle θ is not significant on diagonal frequencies (ω_{ii}, $i=j$), it is quite significant on the cross (non-diagonal) frequencies (ω_{ij}, $i \neq j$). It can be seen also that the higher the frequency, the lower the down-shift caused by damage. It should be noted that in the initial isotropic undamaged state, the cross frequencies (ω_{ij}, $i \neq j$) have the same magnitude both for *ij*-th mode and *ji*-th mode. When anisotropic damage occurs, these cross frequencies are shifted by different magnitudes and hence they attain different values (such that ω_{12} and ω_{21}) due to the non-symmetric property of the net shear stresses (Valliappan *et al.* 1990), $\tau_{ij}^* \neq \tau_{ji}^*$. However, when the damage angle reaches 45°, the cross frequencies have the same values again.

This particular simulation may be used to identify the state of isotropic and anisotropic damage in a structural component. From the results presented in this section, the following observations can be made about the behaviour of damaged vibrating structures:

1. The frequency spectrum is down-shifted for all modes;
2. If the damage is isotropic, the frequency spectrum of the structure is uniformly down-shifted;
3. However, if the damage is anisotropic, the frequency spectrum shift exhibits an anisotropic behaviour and generates different coupled cross frequencies;
4. The influence of damage angle (θ) on the principal (diagonal) frequencies (ω_{ii}) is not as significant as in the case of the cross (non diagonal) frequencies (ω_{ij}).

As a result, it may be possible to perform a back analysis for a damaged structure by inspecting its frequencies in the damaged state. By measuring the frequency shifts of damaged structure, the anisotropic damage state may be investigated by various parametric studies.

6.2. Influence of damage on damping ratio

In order to study the influence of damage on the damping ratio of materials, the history of the amplitude decrements of the cantilever beam has been recorded. The procedure of the Logarithmic Decrement Method to measure the damping of the cantilever beam (Meirovitch 1975) has been numerically simulated for various damage states. Fig. 15 shows the simulated damage factor effects on the damping ratio η_ζ for various damage states 0-0.8.

Fig. 16 shows how the damage factor for damping ratio η_ζ, viscous damping η_γ and critical damping $\eta_{\gamma c}$ (Zhang 1992) vary with the damage variable Ω for the cantilever beam where ω_1/ω_2= 0.1596. From this figure, it can be seen that the damping ratio ζ^* increases significantly, whereas the equivalent viscous damping and critical damping decrease when damage growth occurs. The reason for this is that the natural frequency is decreasing significantly and critical damping also decreases much more than viscous damping.

6.3. Influence of damage on magnification factor

From the engineering point of view, the steady-state response at a point in a structure subject to harmonic vibrations can be simplified as the response of an equivalent mass-spring system with a single degree of freedom. The mass should be taken as an equivalent mass, and the stiffness should be taken as an equivalent stiffness by Rayleigh's method. Thus, the dynamic response magnification factor for a damaged structure can be investigated under various damage states.

Figs. 17(a) and (b) show a comparison of the well-known magnification factor (Meirovitch 1975)

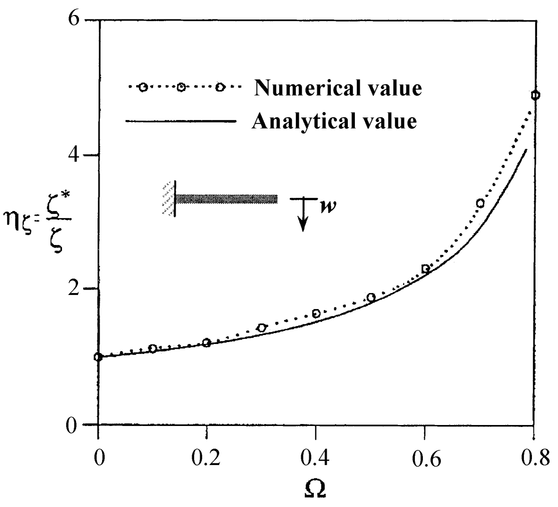

Fig. 15 Comparison of damage factor of damping ratio η_ζ versus damage Ω

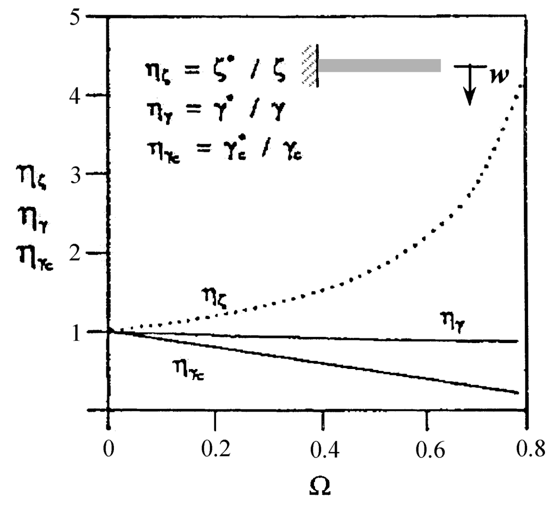

Fig. 16 Damage factor for damping ratio, viscous damping and critical damping versus damage variable

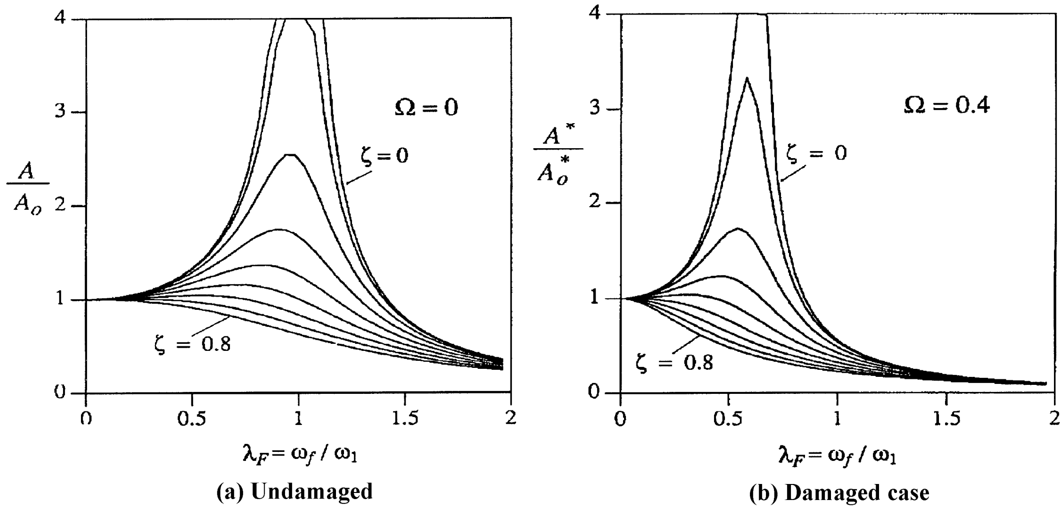

Fig. 17 Comparison of magnification factor between damaged and undamaged cases for various damping ratios ζ=0~0.8

for the cantilever beam in both damaged and undamaged cases against the frequency ratio, ω_f/ω_1, for various damping ratios ζ=0~0.8. It can be seen that the resonance peak moves forward and decreases with the damage. This means that, even though the excitation frequency ω_f is less than the basic natural frequency ω_1, a resonant response may become possible in a damaged structure.

6.4. Influence of damage on phase angle

The other influence of damage on the dynamic response of a structure is the phase angle. The

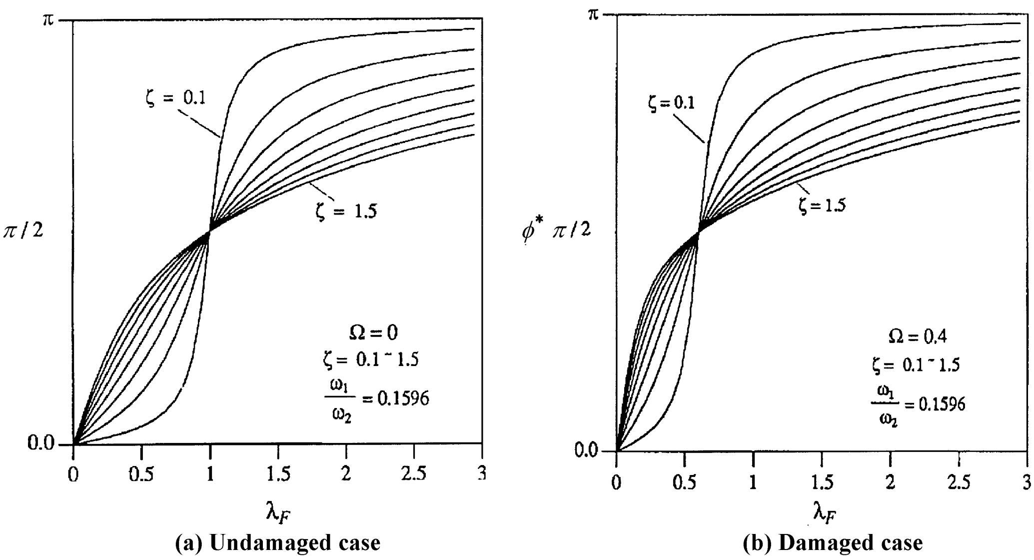

Fig. 18 Comparison of phase angle between damaged and undamaged cases

phase angle of the equivalent system is defined as $\phi = \arctan(2\zeta\ \lambda_F/1-\lambda_F^2)$ (Meirovitch 1975). Similarly, a damaged phase angle ϕ^* can be introduced for damaged material.

Figs. 18(a) and (b) show the plots of the different undamaged and damaged phase angles, when the damping ratio varies from 0.1 to 1.5. Comparing Figs. 18(a) and (b), it can be seen that for the case of damage variable 0.4, the "*invariant point*" of resonance in the phase plane, $\phi \sim \lambda_F$, is shifted from $\lambda_F=1$ (undamaged case) to $\lambda_F=0.65$.

7. Conclusions

In this study, analytical models describing the effects that damage has on the dynamic response of a structural element and the damage behaviour of damaged materials have been developed in both the isotropic and anisotropic cases using the finite element technique. From the results of the analysis, the following conclusions can be drawn:

When a damaged structure is subjected to dynamic loading, because of higher stresses near the damaged areas, the dynamic response increases significantly with the degree of damage and this in turn influences the damage propagation. Further, the natural frequencies are reduced significantly with the damage growth. For damaged materials, it has been found that the damping ratio increases significantly while the equivalent viscous damping and critical damping decrease when a damage growth occurs. Moreover, it was noted that the damage growth may turn the response of a structure into resonance and as soon as a damage-induced resonance occurs, the stress level increases and the damage grows even faster.

From the numerical investigation of the dynamic properties of simple damaged structures (like cantilever beams, deep beams and square plates) the understanding of the influence of the damage and its growth on the frequency, amplitude, phase angle, response, resonance and material damping of dynamic systems was gained. This gives the possibility of working out a method for controlling the damage and its growth in a damaged material, as well the dynamic response of a damaged structure .

Acknowledgements

The financial supports from the Science and Technology Development Research Fund by Zhejiang Province in China and the Fund for Returned Abroad Scholar of China by Chinese Educational Committee are gratefully acknowledged.

References

Audoin, B. and Baste, D. (1994), "Ultrasonic evaluation of stiffness tensor changes and associated anisotropic damage in a ceramic matrix Composite", *J. of Applied Mechanics,* **61**, 309-316.

Cordebois, J.P. and Sidoroff, F. (1982), *Damage Induced Elastic Anisotropy*, Edited by Boehler J., Martinus Nijhoff, The Hague, 761-774.

Fahrenthold, E.P. (1991), "A continuum damage model for fracture of brittle solids under dynamic loading", *J. of Appl. Mech., ASME*, **58**, 904-909.

Gamby, D., Lafarie-Frenot, M. and Henaff-Gardin, C. (1997), "Kinematic wave and non-uniform damage

development in composite laminates", *Int. J. Damage Mech.*, **l6**, 51-61.
Kachanov, L.M. (1986), *Introduction to Continuum Damage Mechanics*, Martinus Nijhoff Publishers, Brookline MA02146, USA.
Kawamoto, T., Ichikawa, Y. and Kyoya, T. (1988), "Deformation and fracturing behaviour of discontinuous rock mass and damage mechanics theory", *Int. J. for Numerical and Analytical Methods in Geomechanics*, **12**, 1-30.
Marigo, J.J. (1985), "Modelling of brittle and fatigue damage for elastic material by growth of microvoids", *J. Engg. Fracture Mech.* **21**, 861-874.
Meirovitch, L. (1975), *Elements of Vibration Analysis*, McGraw-Hill, New York.
Pendey, A.K. and Biswas, M. (1994), "Damage detection in structures using changes in flexibility", *J. Sound and Vibrations*, **169**(1), 3-17.
Valliappan, S., Zhang Wohua and Murti, V. (1990), "Finite element analysis of anisotropic damage mechanics problems", *J. Engg. Fracture Mech.*, **35**, 1061-1076.
Valliappan, S. and Zhang Wohua, (1993), "Dynamic analysis of rock engineering problems based on damage mechanics", *Int. Symp. on Application of Computer Methods in Rock Mechanics and Engineering*, Xian Institute of Mining and Tech., China, 268-373.
Valliappan, S. and Zhang Wohua, (1996), "Analysis of structural components based on damage mechanics concept", *Current Advances in Mechanical Design and Production*, Eds., Elarabi and Wifi, Pergamen Press, 265-280.
Wang Yue-cong, (1993), "Modeling of damping in transient dynamic finite element analysis", Ph.D. Thesis, University of New South Wales, Australia.
Zhang Wohua, (1992), "Numerical analysis of continuum damage mechanics", Ph.D. Thesis, University of New South Wales, Australia.
Zhang Wohua, (1993), "Fatigue damage analysis of hammer foundation", *Proc. of Seminar on Impact of Computational Mechanics on Engineering Problems*, Ed. by Pulmano, A.A. BALKEMA Publishers. 167-174.
Zhang Wohua and Valliappan, S. (1998), "Continuum damage mechanics theory and application, Part I: Theory; Part II: Application", *Int. J. of Damage Mech.*, **7**, 250-273, 274-297.
Zhang Wohua and Valliappan, S. (1990), "Analysis of random anisotropic damage mechanics problems of rock mass, Part I: Probabilistic simulation; Part II: Statistical estimation", *Int. J. Rock Mech. and Rock Engg.*, **23**, 91-112, 241-259.